JOURNAL OF MATERIALS SCIENCE 30 (1995) 552–560

Thermal stresses and strains in injection moulding: experiments and computations

O. DENIZART, M. VINCENT, J. F. AGASSANT
Centre de Mise en Forme des Matériaux, URA CNRS n 1374, Ecole des Mines de Paris BP 207, 06904 Sophia-Antipolis Cedex, France

The effect of thermal stresses in moulded components has been demonstrated by measuring the warpage of centre-gated discs which were injected in a mould, the two sides of which were regulated at different temperatures. Polypropylene discs exhibited larger warpage than polystyrene ones. The measured curvature increased with the difference in mould temperature, and decreased when the packing pressure increased. Thermal stresses and strains have been computed assuming an orthotropic thermo-elastic behaviour for the polymer. A three-dimensional finite element method was used. The different steps of the moulding process, and associated changes of boundary conditions, have been taken into account. The results are qualitatively in agreement with the measurements. Finally the calculation was applied to a box mould, leading to a characteristic box deformation in "diamond ace" form which is consistent with the experiments.

1. Introduction

The existence of residual stresses and strains is a critical problem encountered in injection moulding of thermoplastic polymers: the shape of the part after demoulding differs from the shape of the mould cavity and it can change during its life (during a painting operation or when the temperature is significantly modified). In addition, a too high level of residual stresses can diminish the impact resistance of the part.

The general term "residual stresses" may, in fact, hide different kinds of phenomena such as frozen-in orientation, flow stresses or thermal stresses. In injection moulding, the mechanisms which will promote these different residual stresses are often similar, which does not facilitate their analysis:

(a) The macromolecular orientation is linked to the shear and elongational stresses developed during the filling and the packing stages of the mould, and it is partly frozen-in because of the rapid cooling;

(b) the temperature profile during packing and cooling is linked to the conduction heat transfer between the cooled mould walls and the hot molten polymer, and also to the heat dissipation induced by flow stresses during mould filling. Therefore, thermal shrinkage is different over the part, leading to thermal stresses and warpage after ejection;

(c) in addition, macromolecular orientation as well as crystallization in the case of semicrystalline polymers will be different throughout the thickness of the part, because of the different stresses and cooling rates. This will induce heterogeneity within the part thickness as well as anisotropy between the direction of the flow and the cross-flow direction of mechanical properties and thermal expansion coefficient.

In the present work the effect of thermal residual stresses in disc parts submitted to asymmetric cooling was investigated measuring the warpage of the disc. A three-dimensional temperature dependent thermo-elastic finite element model, taking into account heterogeneous and anisotropic values for the thermal expansion coefficient and for the Young's modulus, is presented here. The numerical results are compared to the experiments. Finally, this model is applied to understand shrinkage and warpage phenomena in a box-shaped mould.

2. Experimental procedure

2.1. Measurements of residual stresses: state of the art

Destructive as well as non-destructive methods have been used for several decades in order to measure residual stresses in different kinds of materials (glass, metals and, more recently, polymers).

2.1.1. Non-destructive methods

Photoelasticity is a well-known technique for measuring the stress state in complex parts subjected to external forces using a transparent polymer scale model. Vincent *et al.* [1] measured directly thermal stresses in polyethylene submarine cable coating. This technique is difficult to use in injection moulding, because it averages macromolecular orientation and thermal stresses (in extrusion, especially for the large thicknesses encountered in submarine cable coating, the orientation phenomena are negligible). In addition, the largest stress gradients are located in the part thickness and their observation makes a preliminary destructive cutting operation necessary. X-ray diffraction has been used to measure residual stresses in metal parts. It may also be applied for highly

0022–2461

crystalline polymers. For amorphous polymers, Barrett and Predecki [2] introduced small metallic particles in the polymer, then measured their lattice deformation in the injected part and therefore deduced the stress state in the polymer material assuming a perfect contact between metallic particles and matrix.

Asymmetric cooling consists in regulating the two sides of a plaque or of a disc mould at distinct temperatures. When demoulded, the plaque or the disc is warped and the radius of curvature may be measured at different time steps. It is related to the stress state throughout the thickness of the part. Several preliminary measurements have been performed by St Jacques [3] and by Riess [4].

2.1.2. Destructive methods

The stress relaxation method consists in measuring the kinetics of stress relaxation which depends on the level of residual stresses [5, 6]. The main disadvantage of this method is that only average through-thickness stresses are measured. In the so-called hole-drilling method, a hole is machined at the surface of a part, the deformations around the hole are measured at the surface by strain gauges and the stress state is then deduced. This method has been intensively used in metal parts. Ito [7] tried to transpose the technique to thermoplastic parts with great experimental difficulties, among which were the appearance of cracks around the hole, and the introduction of stress by machining. The most popular method for thermoplastic parts is the so-called "layer removal method" which consists in cutting a sample within the injected part, then removing successive layers in this sample, at each step measuring the radius of curvature of the remaining part of the sample, and finally calculating the stress state throughout the thickness using the Treuting and Read [8] equation. Even though this technique is very attractive because it leads to the stress profile throughout the thickness of the part, it must be remembered that it is based on restrictive assumptions: (1) the stress state is not modified by the cutting operation, (2) the layer removal operation does not modify the stress state (before warping), (3) the stress state is homogeneous in the plane of the sample, (4) the material is homogeneous and isotropic, (5) the material has a purely elastic behaviour and the sample is submitted to pure bending. This method has been used by Isayev and Crouthamel [9] to study the influence of the injection parameters on the stress state. One of the key points in this method is the time elapsed between the layer removal and the measurement of the radius of curvature. Isayev and Crouthamel tried to reduce this time to a minimum (2 min in the best situation), whereas Siegman *et al.* [10] waited until the radius of curvature reached its maximum value.

2.2. Polymers and moulds

Two commercially available polymers were used, a polystyrene Gedex 1541 from Norsolor (now Elf-Atochem) and a polypropylene 3050 MN4 from Elf-Atochem. Several centre-gated disc moulds with different diameters and thicknesses were used (Table I) under different injection parameters (flow rate, mould temperature, packing pressure, packing time, etc.). They will be indicated when presenting the different experimental tests.

2.3. Warpage measurements in asymmetric cooling experiments

Two successive sets of experiments were performed. The first one was performed with Disc 2 mould geometry (see Table I): two disc thicknesses were tested (2 and 4 mm). Polystyrene and polypropylene were injected with different temperature gradients between the upper and lower parts of the mould (T_{m_1} and T_{m_2}) and different packing pressures (see Table II). The shape of the part after demoulding was measured by

TABLE I The different disc mould geometries

Name	Diameter (mm)	Thickness (mm)	Origin
Disc 1	160	3	Elf-atochem
Disc 2	360	2	Elf-Atochem
		4	
Disc 3	110	2	Lycée Technique d'Oyonnax

TABLE II Asymmetric cooling experiments: injection moulding conditions for Disc 2 polystyrene and polypropylene samples

Polymer	Flow rate ($m^3 s^{-1}$)	Polymer temperature (°C)	Mould temperature, T_{m1}/T_{m2} (°C)	Packing pressure (MPa)
Polystyrene	7×10^{-5}	220	30/30	40
			65/65	40
			65/30	25
			65/30	40
			65/30	65
Polypropylene	5.5×10^{-5}	230	30/30	40
			65/65	40
			65/30	25
			65/30	40
			65/30	65

SEVA mould manufacturing company using a three dimensional contactless measuring system. The position of 60 points was compared to a reference point. The delay between injection and shape measurement was about 3 months. The temperature of the disc was kept constant at 25 °C during this period.

When symmetric cooling temperature are used the shape of the disc is supposed to remain flat. In fact, warpage was observed. This may be related to the non-symmetrical location of the mould sprue as well as to preferential detachment of the part from one side of the mould. The same kind of phenomenon has been observed by Hecini [11] on a plaque geometry. It remains limited for polystyrene (Fig. 1a) but is more pronounced for polypropylene (Fig. 1b). This may be related to the higher thermal expansion coefficient ($22 \times 10^{-5}\,°C^{-1}$ instead of $5 \times 10^{-5}\,°C^{-1}$) for polypropylene. The conclusions are similar for the 2 and 4 mm thick discs. Note that the scale is not identical in the plane of the part and in the thickness direction.

When asymmetric cooling is used, warpage is significantly enhanced. This is clearly shown in Fig. 2 for polypropylene Disc 2, 4 mm thick. When increasing the packing pressure for given mould temperatures (65/30 °C), the curvature of polypropylene discs decreases significantly (Fig. 3).

The second set of experiments was performed with Disc 3 mould geometry (see Table I). Polystyrene was injected with the same flow rate, $9 \times 10^{-5}\ m^3\,s^{-1}$, and

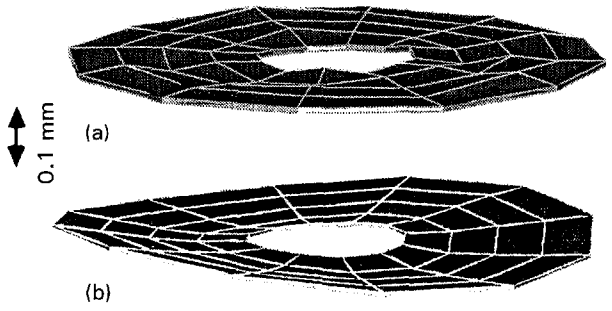

Figure 1 Warpage effects for polystyrene (a) and (b) polypropylene 2 mm thick discs (Disc 2) injected under the same conditions (packing pressure 40 MPa) and with equal upper and lower mould temperatures (30 °C).

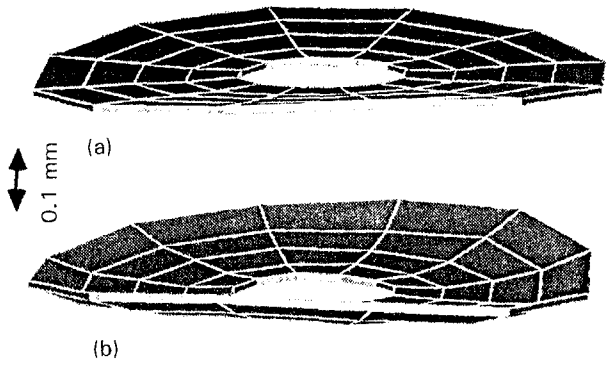

Figure 2 Warpage effects for polypropylene Disc 2, 4 mm thick: (a) symmetric cooling conditions (30/30 °C); (b) non-symmetric cooling conditions (65/30 °C); other injection parameters were kept constant (packing pressure 40 MPa).

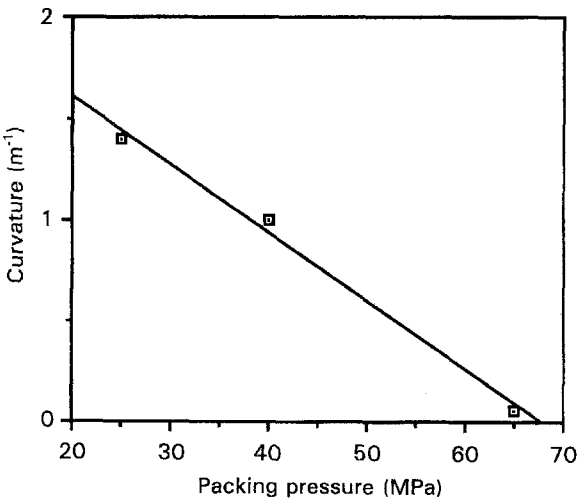

Figure 3 Influence of the packing pressure on the curvature of polypropylene Disc 2, 4 mm thick; mould temperatures 65/30 °C, other injection parameters were kept constant (see Table II).

melt temperature, 240 °C, with different temperature gradients between the upper and lower mould walls. The influence of the packing pressure, the packing holding time, and two cooling procedures after ejection, in air at 25 °C or in water at 5 °C, was tested. The radius of curvature was measured with a three-dimensional profilometer. The time elapsed between injection moulding and measurement was 1 week. The discs were kept at a constant temperature (room temperature for the samples which were cooled at ambient temperature, − 15 °C for the samples quenched in water). When increasing the temperature gradient, the curvature increases (Fig. 4a). It is interesting to note that the sign of the curvature changes when the temperature gradient is inverted, which indicates that there is no significant stiffening effect of the mould sprue. The influence of the temperature gradient is enhanced when the disc is quenched in water at 5 °C which demonstrates the existence of stress relaxation phenomena during cooling. When increasing the packing pressure, the curvature decreases (Fig. 4b) as pointed out previously with Disc 2 experiments. The curvature decreases when the packing holding time and the cooling time increase.

These experiments clearly show the influence of the packing pressure and cooling conditions on part warpage and thus on residual stresses.

3. Computation of the thermal stresses

3.1. State of the art

The first models dealing with thermal stresses were developed for glass forming. Bartenev [12] considered the quenching operation of an infinite plane plaque. He developed a thermo-elastic model with a fictitious parameter to account for glass solidification. Aggarwala and Saibel [13], Lee and Rogers [14] and Crochet and Denayer [15] introduced more sophisticated thermo-viscoelastic material behaviours. The quenching of an infinite polymer thermoplastic plane plaque has been first analysed by Righdal [16] using a thermo-elastic model and by Struik [17] and Aarab

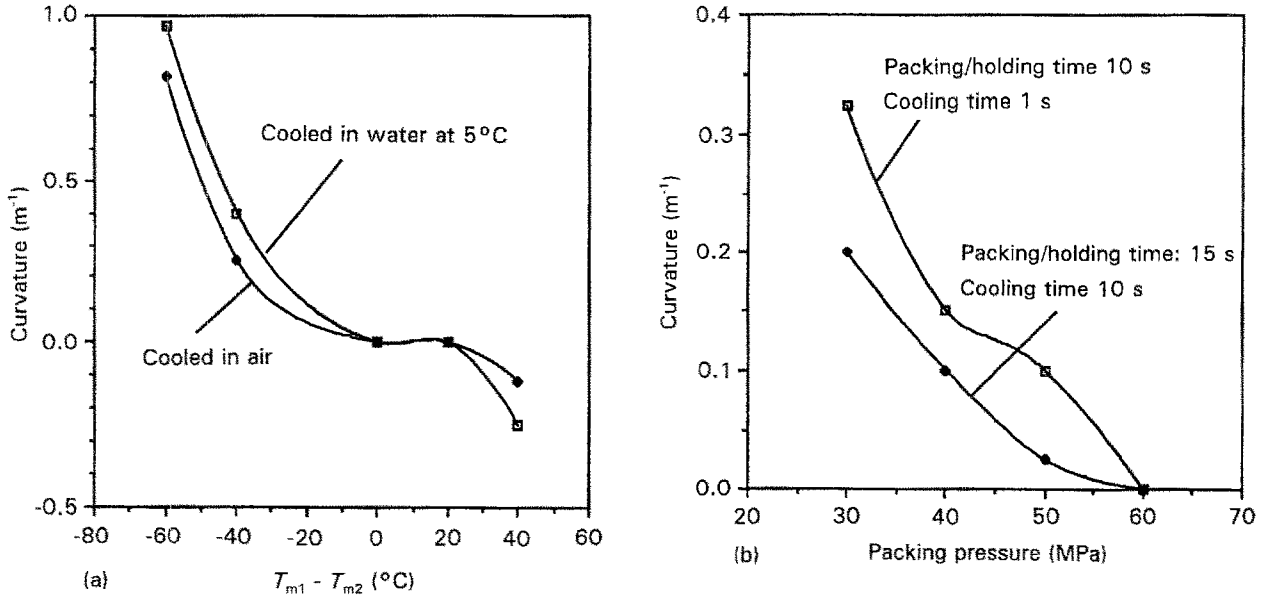

Figure 4 Polystyrene Disc 3: (a) curvature as a function of the temperature gradient (packing pressure 30 MPa); (b) curvature as a function of the packing pressure (the disc has been cooled in air, temperature gradient 40 °C).

[18] for thermo-viscoelastic models. When dealing with injection moulding, the problem is much more complex because of the influence of the thermo-mechanical history (mould filling and packing) and of the modifications of the boundary conditions during the injection cycle (closed, then open mould). Menges *et al.* [19] developed the well-known layer method which consists in dividing the flat sample in several fictitious slices (with well-defined thermoelastic parameters) and in considering a homogeneous deformation for the whole sample (free or blocked, depending on the geometry of the injected part). Mills [20] took into account the packing parameters (packing pressure and packing holding time, freezing time of the mould sprue). Ries [4] improved the Menges model especially by taking into account a thermo-viscoelastic behaviour and the modification of the boundary conditions after demoulding. Titomanlio *et al.* [21] analysed carefully the phase transitions during packing. More recently, Baaijens [22] and Kabanemi and Crochet [23] proposed integrated models including the filling and packing phases for more general geometries and thermo-viscoelastic equations.

Our model takes into account three-dimensional geometries, heterogeneous and non-isotropic temperature-dependent thermoelastic parameters, the influence of the filling and the packing stages, as well as the modification of the boundary conditions after demoulding.

3.2. The incremental thermo-elastic computation

The succesive injection steps are shown in Fig. 5.

(a) The filling stage: the temperature field and the solid-layer thickness distribution at the end of the filling stage have been determined using the injection moulding software FILL2 (see Agassant *et al.* [24]). End of filling will be considered as the initial time for

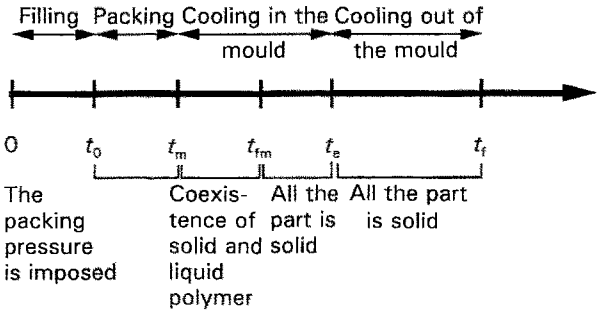

Figure 5 Characteristic times of the injection process.

the development of the thermal stresses in the injected part, which means that the thermal stresses in the two thin solidified layers along the mould walls at the end of the filling stage have been neglected.

(b) The packing stage: during this stage, the pressure in the liquid is imposed by the machine until the gate solidification. It is supposed to remain homogeneous in all the liquid area. Only the cooling mechanism has been considered in this paper. The thermal balance equation is

$$\rho c\,(T)\frac{\mathrm{d}T}{\mathrm{d}t} = \mathrm{div}\,(k\ \mathrm{grad}\ T) \qquad (1)$$

The viscous dissipation has been neglected during the packing stage, as well as the influence of the pressure on the internal energy. For semi-crystalline polymers, the enthalpy of crystallization has been taken into account in the volumic thermal capacity $\rho c(T)$. The polymer has been considered to be solidified when $T < T^*$ (T^* is a no-flow temperature for amorphous polymers and a crystallization temperature for semi-crystalline polymers).

Because the gate is not frozen, the thermal shrinkage in the liquid area is neglected because it is compensated by the entrance of molten polymer due to the packing pressure.

In the solidified layer, an incremental thermo-elastic approach (Equation 2) is used to calculate the deformation

$$\Delta\varepsilon^{\text{total}} = S\Delta\sigma + [S(T+\Delta T) - S(T)]\sigma(t) + \int_{T}^{T+\Delta T} \alpha(T')\, I_d \mathrm{d}T' \quad (2)$$

where S is the orthotropic elastic compliance tensor, α the orthotropic thermal expansion tensor, σ the stress tensor at time t (when the temperature distribution is T) and $\Delta\sigma$ is the stress increment between t and $t + \mathrm{d}t$ (when the temperature distribution is $T + \Delta T$).

The deformation of the mould is neglected and a perfect contact between the solidified layers and the mould is considered. A constant isotropic pressure equal to the packing pressure is considered at the liquid–solid interface.

(c) The cooling stage in the mould: the same incremental thermoelastic approach (Equation 2) is used but now both in the melt pool and in the solidified layers until time t_{fm} and in the whole solid part between time t_{fm} and the demoulding time, t_e. A perfect contact is considered between the mould wall and the polymer. When molten and solid polymer are present simultaneously, the pressure in the melt is imposed as a boundary condition at the solid–liquid interface. This pressure decreases progressively following Equation 3

$$\Delta P = \frac{\Delta V}{\chi V} \quad (3)$$

where χ is the compressibility coefficient of the molten polymer and ΔV is the volume change induced by the thermal shrinkage (Equation 4)

$$\Delta V = \int_{\Omega} \mathrm{tr}\alpha\, \Delta T\, \mathrm{d}v \quad (4)$$

where Ω is the volume of the part.

(d) Demoulding ($t = t_e$): the boundary conditions are suddenly modified (zero stress instead of zero deformation) and a purely elastic instantaneous deformation is considered at the temperature field existing in the part at demoulding time.

(e) The cooling stage out of the mould: zero-stress boundary conditions are considered at the periphery of the part. Free-convection thermal boundary conditions are considered when the part is cooled in air at ambient temperature. The temperature of the fluid is imposed at the part surface when quenching in water. The thermo-elastic temperature-dependent incremental formulation is used in order to account for large deformations of the part. If the deformation of the part remains small, the stress development during this cooling stage can be performed in one step.

3.3. Finite element formulation

(a) Thermo-elastic formulation: at each time step, the increment of displacement Δu is obtained by minimizing the functional $\Phi(\Delta u)$

$$\Phi(\Delta u) = \frac{1}{2}\int_{\Omega} \Delta\sigma : \Delta\varepsilon \mathrm{d}v - \int_{\Omega} S^{-1}(\alpha\Delta T + \Delta S\, \sigma_{\text{int}}) : \Delta\varepsilon \mathrm{d}v \quad (5)$$

where $\Delta\sigma$ is the incremental stress step related to the incremental deformation, $\Delta\varepsilon$, defined by Equation 2. σ_{int} is the stress distribution at time t. Owing to the large deformation encountered during the cooling stage out of the mould, a Newton Raphson algorithm has been used in order to ensure, at each time step, the mechanical equilibrium on the final configuration.

(b) Thermal formulation: the thermal balance (Equation 1) has been solved using a three-dimensional software package which has been developed in our laboratory (see Soyris, [25]).

(c) General algorithm: at each time step, the new temperature field is computed to determine the thickness of the solid layer. The calculated displacement, Δu, leads to the new geometry, defined by the position x of the material points, by

$$x = x + \Delta u \quad (6)$$

and the new stress state by

$$\sigma = \sigma + \Delta\sigma \quad (7)$$

The boundary conditions for the displacements, the stresses and the temperature are incrementally modified depending on the chronology of the time increment in comparison with the characteristic steps of the process (see Fig. 5).

3.4. Applications

(a) Disc 1 geometry filled with polystyrene Gedex 1541 was tested with symmetric cooling. The injection parameters were: flow rate $9 \times 10^{-5}\ \mathrm{m^3\,s^{-1}}$; injection temperature 240 °C, holding pressure 10 MPa, packing holding time 15 s, cooling time in the mould 60 s.

Initially, a constant value was chosen for the thermal expansion coefficient ($\alpha = 5 \times 10^{-5}\ \mathrm{°C^{-1}}$) and for Poissons coefficient ($\nu = 0.35$). A temperature dependent homogeneous isotropic value of the Young's modulus was considered ($E = 3300$ MPa at 25 °C, $E = 2620$ MPa at 50 °C and $E = 0$ at T*).

A compressive stress was predicted in the skin region and a tensile stress in the core. When increasing the mould temperature, both compressive stresses and tensile stresses decrease (Fig. 6). When increasing the packing pressure (Fig. 7), the compressive and tensile stresses initially decrease. For a high packing pressure ($P_c = 60$ MPa), an inversion of the stress field is calculated: the skin is now in tension and the core is in compression which is in agreement with the computations of Titomanlio *et al.* [21].

Then anisotropic and inhomogeneous values of the Young's modulus and of the thermal expansion coefficient were introduced in the two skin regions the thicknesses of which were one-sixth of the disc thickness and where a sharp macromolecular orientation may be observed: orthotropic values have been considered for the Young's modulus with values parallel

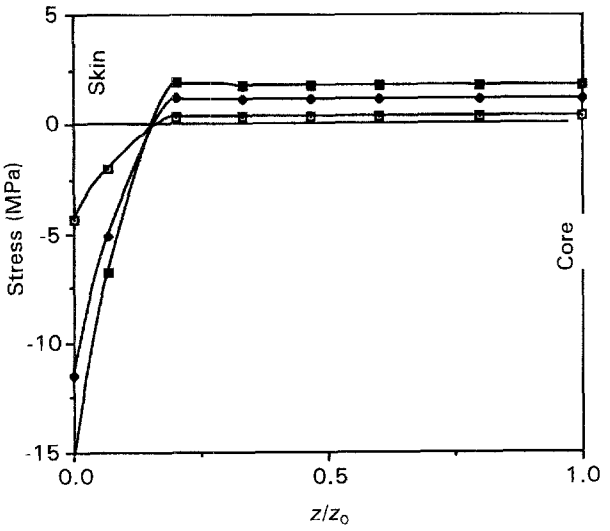

Figure 6 Polystyrene, Disc 1: computed thermal stress distribution throughout the part thickness for three different mould temperatures: (⊡) 75 °C, (◆) 35 °C, (■) 20 °C.

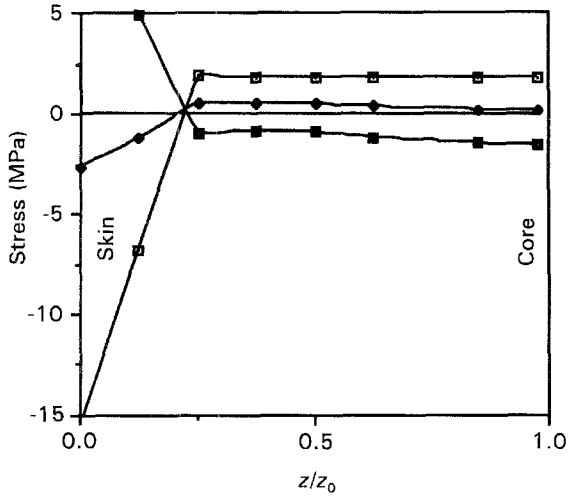

Figure 7 Polystyrene, Disc 1: influence of the packing pressure, P_c: (⊡) 10 MPa, (◆) 30 MPa, (■) 60 MPa. The temperature of the mould is 20 °C.

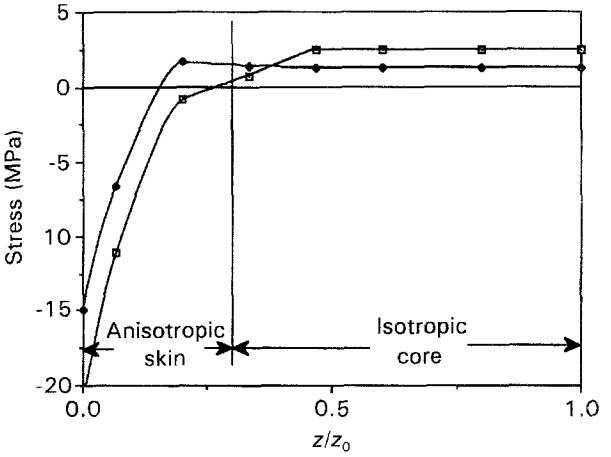

Figure 8 Polystyrene, Disc 1: computed thermal stress distribution throughout the thickness, with anisotropic and inhomogeneous thermo-elastic parameters. (⊡) Radial, (◆) orthoradial.

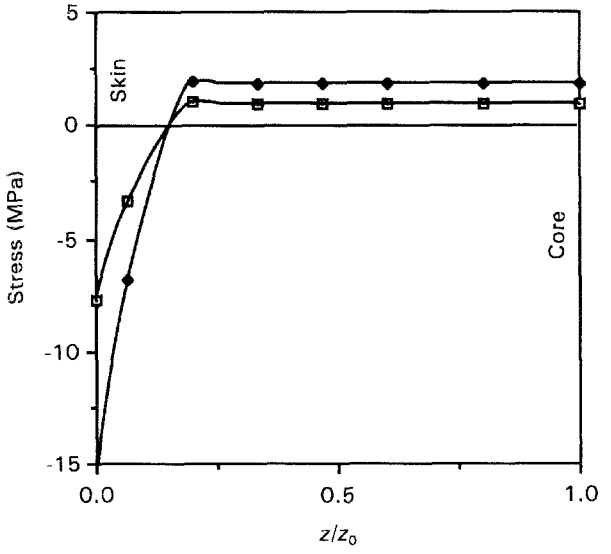

Figure 9 Polystyrene, Disc 1: thermal stress distribution within the thickness for two no-flow temperatures: $T^* =$ (⊡) 100 and (◆) 110 °C.

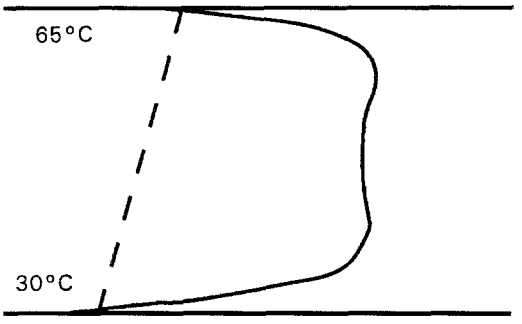

Figure 10 Temperature profile at the end of the filling time throughout the disc thickness.

and perpendicular to the flow equal, respectively, to 4300 and 2800 MPa (at room temperature), and the thermal expansion coefficient with values parallel and perpendicular to the flow equal, respectively, to 3.5×10^{-5} and 5×10^{-5} °C^{-1}. Isotropic values are used in the core region. Such levels of anisotropy have been measured on several polymers by Denizart [26]. The mould temperature was 20 °C. As shown in Fig. 8, stresses are more important in the flow direction than in the direction perpendicular to the flow.

Finally, the influence of the no-flow temperature, T^* was tested. All the preceeding computations were performed with $T^* = 110$ °C. When decreasing the value of T^* to 100 °C the thermal stress distribution was divided by a factor 2 (Fig. 9). Consequently, the influence of small T^* variations is more important than taking into account anisotropic and heterogeneous values for the thermo-elastic parameters.

(b) Disc 2 geometry (thickness 4 mm) filled with polypropylene 3050MN4 was tested with asymmetric cooling (65 °C for the upper wall and 30 °C for the lower one). The initial temperature profile throughout the thickness was uniform in the whole disc (Fig. 10). Isotropic and homogeneous thermo-elastic parameters were considered ($\alpha = 22 \times 10^{-5}$ °C^{-1}, $E = 1300$ MPa and $\nu = 0.4$ at 25 °C. The Young's modulus dependence with temperature was given by Ries [4]). A packing pressure of 20 MPa was imposed for 26 s. Then, the packing pressure was removed and

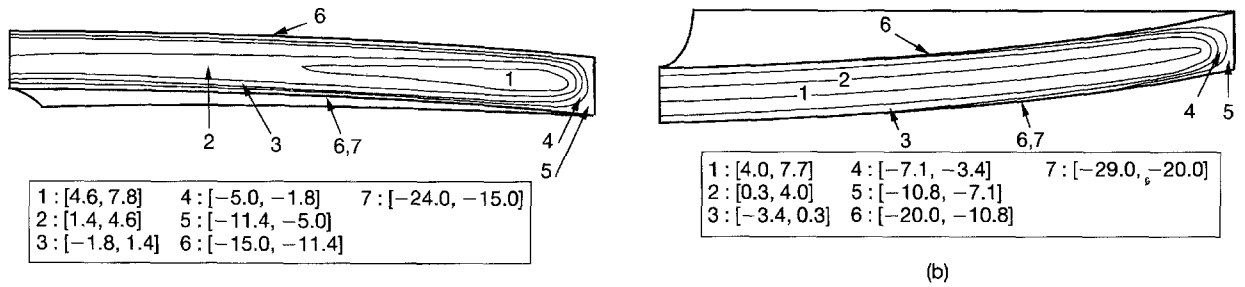

Figure 11 Polypropylene, Disc 2: isovalues of the σ_{rr} stress component (in MPa) and corresponding deformation of the disc: (a) 2 s after demoulding; (b) 15 min after demoulding.

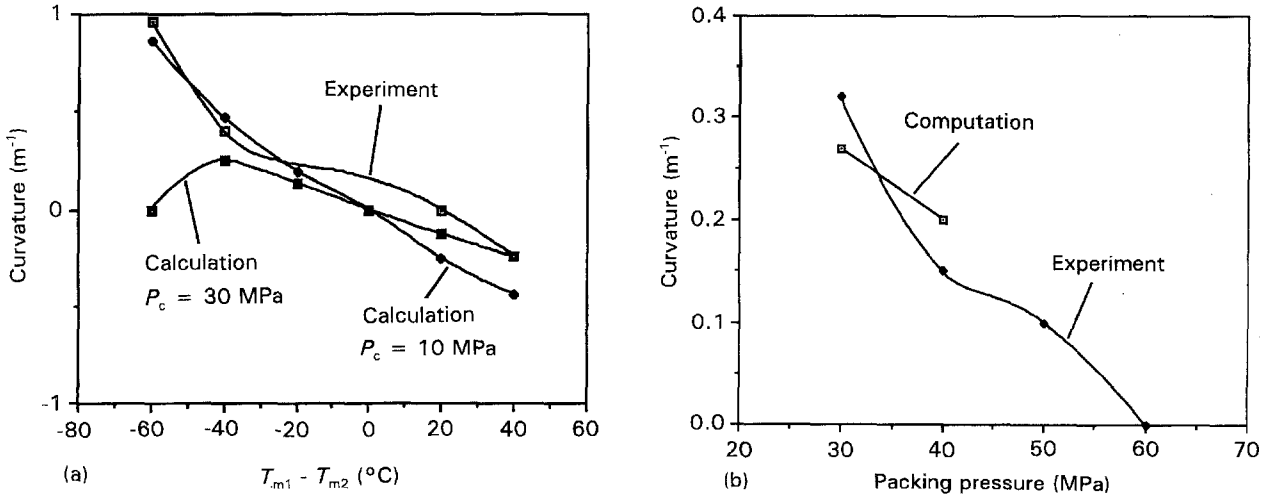

Figure 12 Polystyrene, Disc 3: comparison between computed and experimental curvatures: (a) influence of the mould temperature gradient. Computations are made with two packing pressures, P_c = 30 and 10 MPa; (b) influence of the packing pressure for a temperature gradient of 40 °C.

the disc was successively demoulded and cooled to room temperature.

The temperature and stress fields were incrementally computed, as well as the deformation of the disc. The σ_{zz} component of the stress tensor always remains small in comparison with the σ_{rr} and $\sigma_{\theta\theta}$ components, which are similar. The isovalues of σ_{rr} are represented 2 s after demoulding on Fig. 11a and 15 min after demoulding (when the part is at room temperature) in Fig. 11b. It is interesting to note that the stress field is only slightly modified: tensile stresses are maximum in the core region with a value of 7.8 MPa 2 s after demoulding and 7.7 MPa 15 min after demoulding. The skin is in a compressive state of − 24 MPa 2 s after demoulding and of − 29 MPa 15 min after demoulding toward the cooler side of the mould and of − 15 MPa 2 s after demoulding and − 20 MPa 15 min after demoulding along the warmer side of the mould. It is more interesting to note that the sign of the curvature changes during cooling: the disc is first curved towards the cooler side of the mould and finally curved towards the warmer side of the mould. This is in qualitative agreement with experiments.

4. Comparison between experiments and computation

These comparisons were performed on Disc 3 polystyrene samples. The injection parameters were presented in Section 2.3. The same thermo-elastic data as in the isotropic Disc 1 computations were chosen.

Fig. 12a compares the influence on the curvature of the temperature gradient between the upper and lower parts of the mould. When the computation is performed with a fixed packing pressure P_c = 30 MPa, the agreement is good only for low temperature gradients. When imposing arbitrarily a lower packing pressure, the agreement is good over the whole domain. This may be related to the approximative method used for the computation of the packing stage.

Fig. 12b compares the influence of the packing pressure on the curvature for a constant temperature gradient of 40 °C. The agreement is good at low packing pressure.

As a consequence, the computation model is able to take qualitatively into account the influence of the two more influent parameters we have determined with the asymmetric cooling experiment: the temperature gradient and the packing pressure.

5. Application to a more realistic injected part

A square-box mould was injected at Ecole Nationale Supérieure des Arts et Métiers with a polyamide 6.6 (Rhone Poulenc). The dimensions of the box were 7 cm × 7 cm × 4 cm, with a thickness of 3 mm. The processing conditions were: injection temperature 300 °C,

mould temperature 80 °C, volumic injection rate $Q = 6 \times 10^{-5}\ m^3\ s^{-1}$; packing pressure 30 MPa, packing holding time 10 s, demoulding after 30 s. After demoulding, a characteristic "diamond ace" shape may be observed, as shown in Fig. 13. With the help of a profilometer (which was used for the preceeding asymmetric cooling deformation measurements) a more detailed analysis of the box deformation was performed (Fig. 14): the maximum deflection of the lateral sides of the box was $\delta_1 = 0.76$ mm whereas the deflection of the bottom was $\delta_2 = 0.5$ mm.

A numerical simulation was performed with the following homogeneous and isotropic values for the thermoelastic parameters at room temperature: $E = 1.6$ GPa, $\nu = 0.35$, $\alpha = 2 \times 10^{-4}\ °C^{-1}$. A no-flow temperature $T^* = 260$ °C was chosen.

The deformations after demoulding were computed. For a packing pressure of 10 MPa (lower than the experimental one) the "Diamond ace" defect was predicted (Fig. 15). The computed deflection of the middle of the lateral side with respect to the corner was $\delta_4 - \delta_3 = 0.4$ mm lower than the experimental one (0.76 mm). The computation model does not predict the curvature of the bottom. When increasing the packing pressure to 20 MPa, the warpage values decrease significantly.

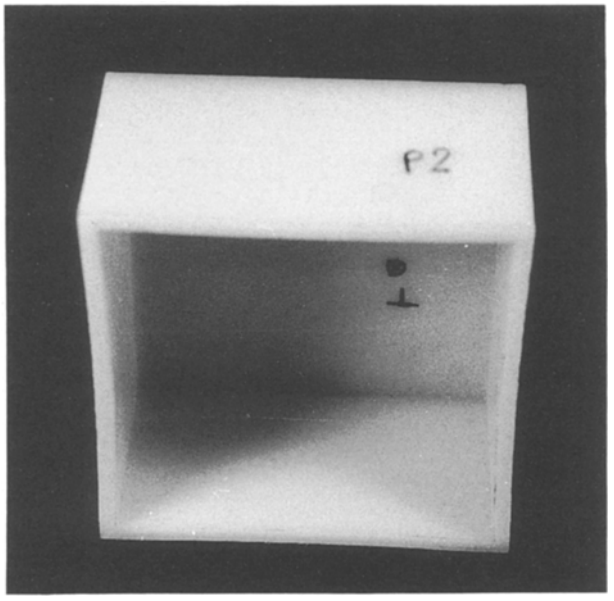

Figure 13 Injected polyamide box.

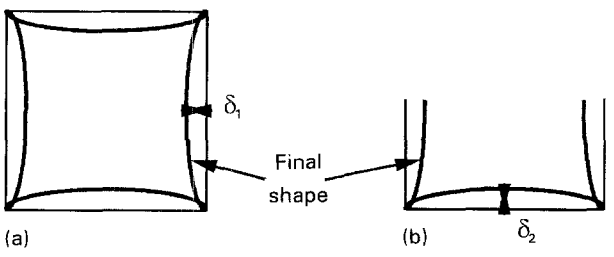

Figure 14 Final shape of the polyamide box: (a) top view, (b) side view.

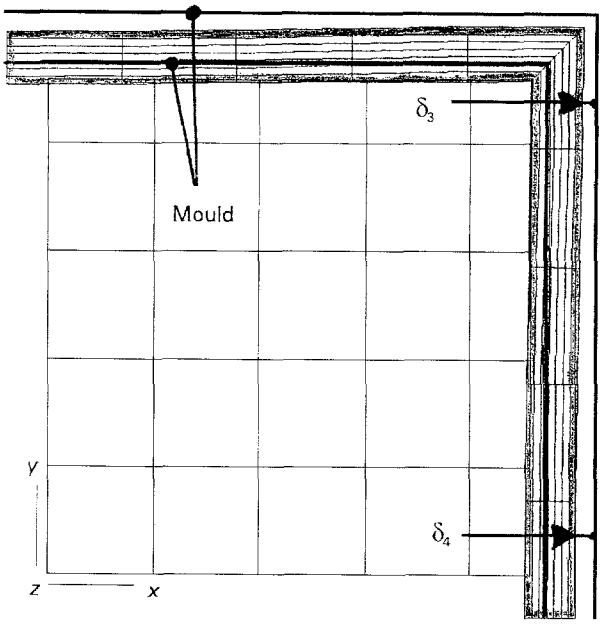

Figure 15 Top view of a quarter of the polyamide box; $\delta_3 = 0.8$ mm, $\delta_4 = 1.2$ mm

6. Conclusions

An asymmetric cooling method has been used in order to show the effect of the residual stress distribution in injected discs. The influence of the temperature gradient between the upper and the lower parts of the mould and of the packing pressure is clearly shown.

A global numerical analysis of the injection moulding process has been built, taking into account the filling stage, the packing stage with a simplified method and the cooling stage inside and outside the mould. A three-dimensional thermo-elastic temperature-dependent finite element method has been proposed for the prediction of the thermal stresses. Heterogeneous and orthotropic values have been tested for the thermoelastic parameters. Careful attention has been devoted to the influence of the characteristic times of the process (packing holding time, frozen time, demoulding time, etc.).

There is a good qualitative agreement between the computation results and the experimental measurements. The influence of the orthotropy and of the heterogeneity of the thermo-elastic parameters seems to be less pronounced than the influence of less intuitive parameters such as the no-flow temperature. At this time, the numerical model appears to be a useful tool to understand shrinkage phenomena in more complex moulds, as it has been shown for a box-shaped part.

For further developments, it will be necessary to improve the model by taking into account more sophisticated phenomena, such as frozen-in flow stresses, more complex boundary conditions, such as mould deformation, contact resistance between the polymer part and the metal of the mould and more realistic thermoviscoelastic constitutive equations. This will require numerous new experimental measurements.

Acknowledgements

This research was supported by the French Ministry for Research and Technology. We are grateful to Norsolor, Elf-Atochem and SEVA companies for technical support in injection moulding and in experimental measurements. We thank our colleagues at the Lycée Technique d'Oyonnax (Professor C. Faure), ENSAM (Professor J.-P. Trotignon), Ecole Polytechnique de Montréal (Professeur P. Lafleur), and CEMEF (Professor J. L. Chenot and Dr. N. Soyris), for technical and numerical assistance.

References

1. M. VINCENT, J. F. AGASSANT, F. X. de CHARENTENAY and A. OUALHA, *J. Méca. Théor. Appl.* **3** (1984) 843.
2. C. S. BARRETT and F. PREDECKI, *Polym. Eng. Sci.* **16** (1976) 9.
3. M. ST JACQUES, *ibid.* **22** (1982) 241.
4. H. RIES, thesis, Institut für Kunststoffverarbeitung, Aachen, Germany (1986).
5. J. C. M. Li, *Canad. J. Phys.* **45** (1967) 493.
6. J. KUBAT and M. RIGDAHL, *Int. J. Polym. Mater.* **3** (1981) 287.
7. K. ITO, *Jpn Plast. Age* **15** (1977) 36.
8. R. G. TREUTING and W. T. READ, *J. Appl. Phys.* **22** (1951) 130.
9. A. I. ISAYEV and D. L. CROUTHAMEL, *Polym. Plast. Tech. Eng.* **22**(2) (1984) 177.
10. A. SIEGMAN, A. BUCHMAN and S. KENIG, *Polym. Eng. Sci.*, **22** (1982) 40.
11. M. HECINI, PhD thesis, Ecole des Arts et Métiers, France (1992).
12. G. M. BARTENEV, *J. Tech. Phys.* **19** (1949) 1423.
13. B. D. AGGARWALA and E. SAIBEL, *Phys. Chem. Glasses* **2** (1961) 137.
14. E. H. LEE and T. G. ROGERS, *J. Appl. Mech.* **30** (1963) 127.
15. M. J. CROCHET and A. DENAYER, *ibid.* **47** (1980) 254.
16. M. RIGHDAL, *Int. J. Polym. Mater.* **5** (1976) 43.
17. L. C. E. STRUIK, *Polym. Eng. Sci.* **18** (1978) 10.
18. A. AARAB, Thesis, Université de Pau et des Pays de l'Adour, France (1982).
19. G. MENGES, A. DIERKES, L. SCHMIDT and E. WINKEL, *SPE ANTEC Tech. Paper* **26** (1980) 300.
20. N. J. MILLS, *Plast. Rubber Proc. Appl.* **3** (1983) 181.
21. G. TITOMANLIO, V. DRUCATO and M. R. KAMAL, *Int. Polym. Proc.* **1** (1987) 55.
22. F. BAAIJENS, *Rheol. Acta* **30** (1991) 284.
23. K. K. KABANEMI and M. J. CROCHET, *Int. Polym. Proc.* **7** (1992) 60.
24. J. F. AGASSANT, H. ALLES, S. PHILIPON and M. VINCENT, *Polym. Eng. Sci.* **28** (1988) 460.
25. N. SOYRIS, PhD thesis, Ecole des Mines de Paris, France (1990).
26. O. DENIZART, PhD thesis, Ecole des Mines de Paris, France (1990).

Received 12 January
and accepted 15 September 1993